World Journal of Gastrointestinal Surgery

Submit a Manuscript: https://www.f6publishing.com

World J Gastrointest Surg 2022 August 27; 14(8): 833-848

DOI: 10.4240/wjgs.v14.i8.833

ISSN 1948-9366 (online)

ORIGINAL ARTICLE

Observational Study

Early detection of colorectal cancer based on circular DNA and common clinical detection indicators

Jian Li, Tao Jiang, Zeng-Ci Ren, Zhen-Lei Wang, Peng-Jun Zhang, Guo-An Xiang

Specialty type: Gastroenterology and hepatology

Provenance and peer review: Unsolicited article; Externally peer reviewed.

Peer-review model: Single blind

Peer-review report's scientific quality classification

Grade A (Excellent): 0
Grade B (Very good): B, B, B
Grade C (Good): 0
Grade D (Fair): 0
Grade E (Poor): 0

P-Reviewer: Andersen JB, Denmark; Bartholomeyczik S, Germany; Groome PA, Canada

Received: April 12, 2022
Peer-review started: April 12, 2022
First decision: May 11, 2022
Revised: May 14, 2022
Accepted: August 6, 2022
Article in press: August 6, 2022
Published online: August 27, 2022

Jian Li, Guo-An Xiang, The Second School of Clinical Medicine, Southern Medical University, Guangzhou 510515, Guangdong Province, China

Jian Li, Guo-An Xiang, Department of General Surgery, Guangdong Second Provincial General Hospital, Guangzhou 510317, Guangdong Province, China

Jian Li, Zeng-Ci Ren, Zhen-Lei Wang, Department of General Surgery, Henan Tumor Hospital, Affiliated Tumor Hospital of Zhengzhou University, Zhengzhou 450000, Henan Province, China

Tao Jiang, Medicine Innovation Research Division of Chinese PLA General Hospital, Beijing 100853, China

Peng-Jun Zhang, Key Laboratory of Carcinogenesis and Translational Research (Ministry of Education/Beijing), Interventional Therapy Department, Peking University Cancer Hospital and Institute, Beijing 100142, China

Corresponding author: Guo-An Xiang, MD, Doctor, The Second School of Clinical Medicine, Southern Medical University, No. 253 Gongye Avenue Haizhu, Guangzhou 510515, Guangdong Province, China. guoanxiang_66@126.com

Abstract

BACKGROUND

Colorectal cancer (CRC) is the third most common cancer worldwide, and it is the second leading cause of death from cancer in the world, accounting for approximately 9% of all cancer deaths. Early detection of CRC is urgently needed in clinical practice.

AIM

To build a multi-parameter diagnostic model for early detection of CRC.

METHODS

Total 59 colorectal polyps (CRP) groups, and 101 CRC patients (38 early-stage CRC and 63 advanced CRC) for model establishment. In addition, 30 CRP groups, and 62 CRC patients (30 early-stage CRC and 32 advanced CRC) were separately included to validate the model. 51 commonly used clinical detection indicators and the 4 extrachromosomal circular DNA markers *NDUFB7*, *CAMK1D*, *PIK3CD* and *PSEN2* that we screened earlier. Four multi-parameter joint analysis methods:

binary logistic regression analysis, discriminant analysis, classification tree and neural network to establish a multi-parameter joint diagnosis model.

RESULTS

Neural network included carcinoembryonic antigen (CEA), ischemia-modified albumin (IMA), sialic acid (SA), *PIK3CD* and lipoprotein a (LPa) was chosen as the optimal multi-parameter combined auxiliary diagnosis model to distinguish CRP and CRC group, when it differentiated 59 CRP and 101 CRC, its overall accuracy was 90.8%, its area under the curve (AUC) was 0.959 (0.934, 0.985), and the sensitivity and specificity were 91.5% and 82.2%, respectively. After validation, when distinguishing based on 30 CRP and 62 CRC patients, the AUC was 0.965 (0.930-1.000), and its sensitivity and specificity were 66.1% and 70.0%. When distinguishing based on 30 CRP and 32 early-stage CRC patients, the AUC was 0.960 (0.916-1.000), with a sensitivity and specificity of 87.5% and 90.0%, distinguishing based on 30 CRP and 30 advanced CRC patients, the AUC was 0.970 (0.936-1.000), with a sensitivity and specificity of 96.7% and 86.7%.

CONCLUSION

We built a multi-parameter neural network diagnostic model included CEA, IMA, SA, *PIK3CD* and LPa for early detection of CRC, compared to the conventional CEA, it showed significant improvement.

Key Words: Colorectal cancer; Colorectal polyps; Multi-parameter; Circular DNA; Neural network

Core Tip: Most patients with colorectal cancer (CRC) are diagnosed at an advanced stage. The high morbidity and mortality of advanced CRC indicates an urgent need for clinical improvements in early CRC detection and individualized management. Compared with free linear DNA, extrachromosomal circular DNA is not easily degraded by nucleases, and its structure is more stable. In this study, we aimed to build a multi-parameter diagnostic model for early detection of CRC.

Citation: Li J, Jiang T, Ren ZC, Wang ZL, Zhang PJ, Xiang GA. Early detection of colorectal cancer based on circular DNA and common clinical detection indicators. *World J Gastrointest Surg* 2022; 14(8): 833-848
URL: https://www.wjgnet.com/1948-9366/full/v14/i8/833.htm
DOI: https://dx.doi.org/10.4240/wjgs.v14.i8.833

INTRODUCTION

Colorectal cancer (CRC) is the third most common cancer worldwide, and it is the second leading cause of death from cancer in the world, accounting for approximately 9% of all cancer deaths. Currently, surgery is the most common treatment for nonmetastatic CRC[1]. Most patients with CRC are diagnosed at an advanced stage. The high morbidity and mortality of advanced CRC indicates an urgent need for clinical improvements in early CRC detection and individualized management[2].

In the era of precision oncology, liquid biopsy has become the primary method for characterizing circulating tumor components present in body fluids[3]. This noninvasive tool can identify relevant molecular alterations in CRC patients, including some that indicate disruption of epigenetic mechanisms. Epigenetic alterations found in solid and liquid biopsies have shown great utility as biomarkers for the early detection, prognosis, monitoring, and assessment of the treatment response in CRC patients[4]. Therefore, the term "liquid biopsy" includes blood, the most commonly used human fluid sample, as well as other fluids, such as urine, ascites, pleural effusion, cerebrospinal fluid, and saliva[5,6]. Both primary tumors and metastases can release tumor material into these body fluids, mainly comprised of circulating tumor cells (CTCs), nucleic acids (cNA), and extracellular vesicles (cEVs)[7]. These circulating elements constitute a valuable source of noninvasive biomarkers[8-11].

At present, single-stranded or double-stranded DNA is detected based on ctDNA. With the development of high-throughput sequencing technology and single-cell gene amplification technology, new types of circular cell-free DNA have been discovered such as extrachromosomal circular DNA (eccDNA)[12,13]. eccDNA refers to a closed circular DNA located outside the chromosome in the form of single-stranded or double-stranded DNA, which is widely found in eukaryotes, including humans [14,15]. Compared with free linear DNA, eccDNA is not easily degraded by nucleases, and its structure is more stable.

In our study, we aimed to build a multi-parameter diagnostic model based on the commonly used clinical detection indicators and the 4 eccDNA markers for early detection of CRC which is urgently needed in clinical practice.

MATERIALS AND METHODS

Study samples

After approval by the ethics committee, the research subjects signed informed consent forms. This project included 59 patients with colorectal polyps (CRP) and 101 CRC patients (38 early-stage CRC and 63 advanced CRC) for building the model. An additional 30 CRP and 62 CRC patients (30 early-stage CRC and 32 advanced CRC) were used to validate the model (Table 1).

The inclusion criteria for the CRP group were those with villous/tubular adenoma, with or without mild-to-moderate hyperplasia, confirmed by colonoscopy and pathologically confirmed after adenoma removal, or confirmed by pathology and immunohistochemistry as focal high-grade neoplasia of villous tubular adenoma. All biochemical examinations and auxiliary examinations showed no abnormality, no complaints of gastrointestinal discomfort, no signs of a tumor, adenoma with a diameter less than 1 cm, no villous adenoma or mixed adenoma, and no adenoma with moderate to severe dysplasia.

In the early CRC group, it was confirmed by tumor surgery that the adenocarcinoma of the intestinal wall was confined to the mucosa or submucosa without lymphatic metastasis, that is, stage 1 or 2, and it was pathologically confirmed villous tubular adenoma with focal high-grade neoplasia or intestinal wall glands.

For the advanced CRC group based on tumor staging according to the American Joint Committee on Cancer tumor node metastasis staging, we defined colorectal cancer stages 3 and 4 as advanced stage with pathologically confirmed colorectal cancer; no treatment was performed before sample collection, including surgery, chemotherapy, radiotherapy, or other treatments; and no blood transfusion had occurred within the past 3 mo.

All enrolled patients provided colorectal cancer or polyp specimens and the corresponding clinical examination data. None of the patients received chemotherapy, radiotherapy or immunotherapy before surgery, and other tumors and gastrointestinal diseases were excluded by examination at the time of admission.

Peripheral blood was collected from all subjects included in this study on an empty stomach in the morning. The anticoagulant in the plasma collection tube was EDTA and after collection, the blood was centrifuged at 3000 rpm for 10 min, and the plasma was placed into a new sterile Eppendorf tube. Serum samples were early morning fasting peripheral blood samples collected in tubes containing separation gel and a clot activator. The samples were centrifuged at 3000 rpm for 10 min, and the serum was transferred to new sterile Eppendorf tubes and stored at -80 °C until assayed. The plasma was also stored at -80 °C. During the sample collection process, hemolyzed and chyle blood samples were removed to avoid repeated freezing and thawing. When testing was conducted, normal temperature recovery was performed.

Detection of commonly used clinical indicators

There were 51 commonly used clinical detection indicators, including 13 common tumor-related markers and 38 clinical biochemical indicators. Among them, 13 tumor-related indicators included carcinoembryonic antigen (CEA), alpha fetoprotein (AFP), carbohydrate antigen 125 (CA125), CA199, CA153, CA724, cytokeratin fragment 211 (Cyfra211), ferritin (Ferr), neuron-specific enolase (NSE), squamous cell carcinoma (SCC), pepsinogen (PG) I, PG II and PGI/II. The 38 clinical biochemical indicators included alanine aminotransferase (ALT), aspartate aminotransferase (AST), total protein (TP), albumin (ALB), total bilirubin (TB), direct bilirubin (DB), total bile acid (TBA), alkaline phosphatase (ALP), γ-glutamyl transfer enzyme (GGT), glucose (GLu), urea nitrogen (UN), creatinine (Cr), uric acid (UA), cholesterol (CHO), triglyceride esters (TG), creatine kinase (CK), lactate dehydrogenase (LDH), creatine kinase isoenzyme (CKMB), calcium (Ca), phosphorus (P), magnesium (Mg), potassium (K), sodium (Na), chlorine (Cl), carbon dioxide (CO_2), lipoprotein a (LPa), high-density lipoprotein (HDL), low-density lipoprotein (LDL), apolipoprotein A1 (ApoA1), apoB, cysteine (CYS), sialic acid (SA), homocysteine (HCY), C-reactive protein (CRP), amylase (AMY), lipase (LPS), superoxide dismutase (SOD) and ischemia-modified albumin (IMA).

Among the 51 detection indicators, CEA, AFP, CA199, CA724, CA125, CA153, Cyfra211, Ferr, NSE, ALT, AST, TP, ALB, ALP, GGT, Glu, UN, CR, UA, CHO, TG, CK, Ca, P, Mg, K, Na, CL, CO2, HDL, LDL, CRP, AMY, and LPS standards and controls and detection kits were purchased from Roche Diagnostics Ltd. ApoA1, ApoB, CYS, LPa, and CKMB standards and controls and detection kits were purchased from Beijing Leadman Biochemical Co., Ltd. SCC, PG I and PG II standards and controls and test kits were purchased from Abbott Diagnostics. TBA and HCY standards and quality controls and detection kits were purchased from Beijing Jiuqiang Biotechnology Co., Ltd. TB and DB standards and controls and assay kits were purchased from Hitachi Diagnostics Co., Ltd. IMA standards, quality control products, and detection kits were purchased from Changsha Yikang Technology Development

Table 1 General clinical characteristics of study subjects

Clinical features	Model building		Model validation	
	CRC (*n* = 101)	CRP (*n* = 59)	CRC (*n* = 62)	CRP (*n* = 30)
Age				
Average	58	56	57	57
Range	29-81	31-76	33-74	35-69
Sex				
Male	60	34	37	19
Female	41	25	25	11
Location				
Ascending colon	21		17	
Descending colon	15		12	
Transverse colon	3		4	
Sigmoid colon	59		28	
Rectal	3		1	
Differentiation				
Well	21		15	
Moderate	57		33	
Poorly	23		14	
TNM stage				
T1	11		11	
T2	27		21	
T3	44		7	
T4	19		23	

CRP: Colorectal polyps; CRC: Colorectal cancer; TNM: Tumor node metastasis.

Co., Ltd. SA standards, quality control products, and detection kits were purchased from Zhejiang Dongou Diagnostic Products Co., Ltd. SOD standards, quality control products and detection kits were purchased from Fujian Fuyuan Biotechnology Co., Ltd. A modular 7600 automatic biochemical analyzer, Roche E170 immunoassay analyzer and Architect i2000 immunoassay system were used to complete the pre-assay quality control and calibration. After the analysis, the experimental data of each instrument were exported for statistical analysis.

Detection of differential eccDNA based on ddPCR

Cell-free DNA was extracted from plasma samples using the QIAamp DNA Blood Kit (Qiagen, 51192) according to the ddPCR detection method established in the second part of this study. ATP-dependent DNase (Epicenter, E310K) was added to the free DNA and digested at 37 °C for 1.5 h to a final concentration of 0.4 U/μL to remove linear double-stranded DNA. The reaction was continued at 70 °C for 30 min to inactivate ATP-dependent DNase activity, and the product was then stored until analysis.

Based on the eccDNA sequence incorporated into the model, primers were designed using Primer3 software. After a homology search was performed with BLAST, the primers were synthesized by Invitrogen. The 5' ends of the primers were modified with a FAM fluorophore, and the 3' ends were modified with a BHQ1 quenching group. (1) *NDUFB7*. Forward sequence: TACCGTCAGCATCCACAGCCAT; reverse sequence: GCCTTCTCAGAAGGATGCCAGT; (2) *CAMK1D*. Forward sequence: TGAGCAGATCCTCAAGGCGGAA; reverse sequence: GTCCTTCTCCATCAGGTTCCGA; (3) *PIK3CD*. Forward sequence: TGCCAAACCACCTCCCATTCCT; reverse sequence: CATCTCGTTGCCGTGGAAAAGC; and (4) *PSEN2*. Forward sequence: GCTGTTTGTGCCTGTCACTCTG; reverse sequence: TGTGTCCTCAGTGAATGGCGTG.

Primers and probes were diluted with deionized water to the storage concentration of 200 μmol/L, and the working concentration was 10 μmol/L. The total PCR volume was 20 μL, including 2-fold ddPCRTTM Super mix 10 μL, forward and reverse primers 1.8 μL each (final concentration 900

nmol/L), probe 0.5 μL (final concentration 250 nmol/L), template DNA 4 μg, and ddH_2O to make it up to 20 μL. Then, 20 μL of the reaction system mixture was added to the droplet generation card for droplet generation. All of the resulting droplets were transferred to a 96-well plate for PCR amplification. The PCR conditions were: 95 °C/10 min; 94 °C/30 s, 60 °C/1 min, 40 cycles; 98 °C/10 min. Finally, Quanta Soft 1.6 software (Bio-Rad, USA) was used to analyze the results and the Flush System was used before each experiment. After the setup is complete, the sample droplets are analyzed. We analyzed the results of the run and view channels, scatterplots, concentration data, ratio data, and the number of events.

Evaluation of the diagnostic value of a single indicator

Second, we compared the 51 common clinical indicators and 4 kinds of eccDNA between the CRP group and CRC group based on the difference indicator, tested by the area under the curve (AUC) and the *P* value, for potential markers to evaluate their diagnostic value for distinguishing the CRP and CRC groups, CRP and early CRC groups, colon polyps and advanced CRC groups.

Establishment and evaluation of the multiparameter diagnosis model

Based on the differential diagnostic value (CRP group *vs* CRC group), we established a multiparameter combined auxiliary diagnostic model. The models are binary logistic regression analysis, discriminant analysis, classification tree and neural network. Binary logistic regression analysis was used for the Forward: Conditional method. Discriminant analysis applied the Bayes discriminant method, and stepwise discriminant analysis was used in the fitting function process. A classification tree was the CHAID classification tree method, and a cross-validation evaluation was conducted to establish the classification tree model. An artificial neural network was the neural network's multilayer perceptron used to build the model.

Validation of the multiparameter diagnosis model

After comparing the diagnostic value of the binary logistic regression analysis, the discriminant analysis, classification tree and neural network with the diagnostic value of a single index were conducted. The optimal multiparameter auxiliary diagnosis model was selected, and 30 CRP groups and 62 CRC patients (30 early-stage CRC patients and 32 advanced CRC patients) were enrolled to validate the multiparameter model. Then, the stability of the model was evaluated. Finally, the validated model was compared with the commonly used clinical detection index CEA, and its clinical application value was evaluated by comparing the sensitivity, specificity, and AUC.

Statistical analysis

SPSS 22.0 was used for statistical analysis. Measurement data were expressed as medians (25%, 75%). If the data were normally distributed, they were compared by two independent samples *t*-tests. If nonnormally distributed, comparisons were made by the rank-sum test. The AUC was used to assess the diagnostic value of the index. Four multiparameter analysis methods (binary logistic regression analysis, discriminant analysis, classification tree and neural network) were used to establish a multiparameter joint diagnosis model. The binary logistic regression model used the forward conditional method. The discriminant analysis used the Bayes discriminant method. The classification tree used the CHAID classification tree method, and the established classification tree model was evaluated by cross-validation. Artificial neural networks used multilayer perceptrons of neural networks to build the models. Univariate and multivariate logistic regression were used to analyze Exp (B) of the index. The *Z* score test was used to compare the AUC of the different groups. $P < 0.05$ indicates that the difference is statistically significant.

RESULTS

Comparison of 51 common clinical indicators and 4 kinds of eccDNA between the colon polyp group and the colorectal cancer group

Thirteen tumor markers (CEA, AFP, CA125, CA199, CA153, CA724, CY211, Ferr, NSE, SCC, PG I/II, PG II, and PG I) and 38 blood biochemical indices (ALT, AST, TP, ALB, TB, DB, TBA, ALP, GGT, GLu, UN, Cr, UA, CHO, TG, CK, LDH, CKMB, Ca, P, Mg, K, Na, Cl, CO_2, LPa, HDL, LDL, ApoA1, ApoB, CYS, SA, HCY, CRP, AMY, LPS, SOD, and IMA) were compared between the 59 CRP patients and the 101 CRC patients. Among the 51 commonly used clinical indicators, 22 indicators, including IMA, CEA, SA, LPa, CK, TB, HDL, NSE, ALT, Ferr, DB, CA125, LDH, AMY, CY211, CA724, HCY, CHO, P, LDL, Cl and CKMB, were significantly different between the CRP and CRC groups ($P < 0.05$). The remaining 29 indicators were not significantly different. By comparison, among the four eccDNA indices, two indices, *CAMK1D* and *PIK3CD*, showed significant differences between the CRP and CRC groups ($P < 0.05$). The other two indicators were not significantly different, as shown in Table 2.

Table 2 Comparison of 51 common clinical indicators between colon polyp group and colorectal cancer group

Index	CRP (*n* = 59)	CRC (*n* = 101)	*F* value	Sig	*P* value
CEA	1.86 (1.17, 2.43)	3.9 (1.67, 13.87)	11.39	< 0.01	< 0.01
AFP	2.58 (1.87, 3.59)	2.41 (1.75, 3.36)	0.02	0.90	0.41
CA125	9.78 (6.77, 13.55)	11.63 (7.98, 19.9)	4.80	0.03	0.04
CA199	8.57 (5.44, 14.38)	13.43 (7.22, 26.48)	3.62	0.06	0.22
CA153	9.5 (7.08, 13.09)	9.25 (6.6, 13)	1.53	0.22	0.49
CA724	1.63 (1.16, 4.39)	2.55 (1.36, 7.33)	5.54	0.02	0.07
CY211	1.82 (1.4, 2.89)	2.3 (1.63, 3.58)	9.29	< 0.01	< 0.01
Ferr	150.9 (85.62, 269.5)	72.12 (17.02, 161.5)	0.11	0.74	0.01
NSE	8.06 (6.52, 9.16)	10 (7.71, 12.63)	4.58	0.03	< 0.01
SCC	1.1 (0.7, 1.5)	0.8 (0.6, 1.2)	2.96	0.09	0.19
PG I/II	4.576 (2.835, 5.914)	5.12 (3.7, 6.53)	0.10	0.76	0.08
PG II	15.9 (9, 28.3)	14.6 (9.7, 24.2)	1.08	0.30	0.64
PG I	75.5 (38.5, 101.3)	71.7 (51.45, 96.3)	0.49	0.49	0.82
ALT	16.8 (12.1, 25)	12.7 (9.3, 17.75)	0.59	0.44	0.03
AST	17.1 (14.1, 20.6)	16.6 (12.25, 19.3)	0.87	0.35	0.43
TP	68.3 (64.1, 71.9)	67.3 (63.15, 70.65)	0.03	0.86	0.29
ALB	41.8 (39.6, 44.4)	39.5 (36.95, 41.45)	0.63	0.43	0.07
TB	12.5 (10, 16.4)	9.7 (7.4, 12.8)	0.75	0.39	< 0.01
DB	4.1 (3.2, 5.2)	3.6 (2.3, 4.2)	0.05	0.82	0.01
TBA	4.2 (2.5, 7.2)	3.5 (2.2, 5.7)	2.15	0.14	0.11
ALP	61.4 (54.8, 73.6)	67 (56.4, 80.05)	2.38	0.13	0.59
GGT	23.6 (13.5, 37.6)	22.3 (14.75, 33.95)	0.01	0.95	0.98
GLu	5.02 (4.79, 5.51)	5.12 (4.74, 5.81)	0.00	0.97	0.97
UN	5.49 (4.64, 6.08)	5.23 (4.08, 6.29)	5.94	0.02	0.43
Cr	70.2 (61.6, 78.6)	65.2 (56.35, 75.6)	0.22	0.64	0.06
UA	312.3 (257.9, 386.9)	292.8 (224, 339.4)	0.19	0.67	0.06
CHO	4.5 (4.04, 5.27)	4.36 (3.88, 5.09)	2.31	0.13	0.02
TG	1.43 (1.01, 2.01)	1.25 (0.93, 1.62)	7.94	0.01	0.45
CK	69.8 (55.5, 118.9)	54.4 (35.2, 71.05)	15.60	< 0.01	0.04
LDH	137 (122.2, 153.3)	148.4 (129.75, 177.75)	4.13	0.04	< 0.01
CKMB	6.6 (4, 9.8)	6.14 (4.05, 9.6)	1.81	0.18	0.02
Ca	2.26 (2.19, 2.31)	2.21 (2.14, 2.27)	0.10	0.75	0.47
P	1.27 (1.14, 1.39)	1.25 (1.07, 1.38)	0.01	0.93	0.01
Mg	0.93 (0.85, 1.01)	0.91 (0.84, 0.97)	0.01	0.94	0.29
K	4.03 (3.78, 4.18)	4.09 (3.87, 4.33)	4.98	0.03	0.53
Na	143.8 (141.6, 145.4)	143.1 (141.45, 144.7)	0.17	0.68	0.12
Cl	105.6 (103.4, 107.2)	105.3 (103.5, 107.4)	2.08	0.15	0.04
CO_2	22.6 (20.7, 26.1)	24.9 (22.9, 26.65)	2.31	0.13	0.40
LPa	7.83 (3.01, 12.74)	15.65 (7.82, 31.65)	13.29	< 0.01	0.01
HDL	1.27 (1.03, 1.41)	1.02 (0.89, 1.23)	0.10	0.76	< 0.01
LDL	2.63 (2.26, 3.28)	2.54 (2.07, 3.27)	1.33	0.25	< 0.01

ApoA1	1.39 (1.17, 1.54)	1.13 (1.01, 1.34)	0.66	0.42	0.55
ApoB	0.83 (0.72, 1.02)	0.83 (0.72, 1.01)	0.09	0.76	0.62
CYS	1.07 (0.95, 1.16)	0.97 (0.84, 1.08)	0.34	0.56	0.70
SA	59.3 (55, 66.5)	67.1 (60.8, 82.4)	13.50	< 0.01	0.04
HCY	15.19 (11.54, 19.68)	13.92 (11.18, 17.42)	4.71	0.03	< 0.01
CRP	0.7 (0.4, 1.5)	3.9 (1, 10.55)	30.41	< 0.01	0.11
AMY	59.5 (50, 73.7)	51.8 (38.95, 64.7)	1.18	0.28	< 0.01
LPS	33.1 (25.1, 42.7)	32.9 (22.25, 44.25)	2.87	0.09	0.06
SOD	136.1 (125, 147)	136.5 (115.8, 156.9)	4.82	0.03	0.35
IMA	63.8 (60.1, 66.3)	62.1 (59.45, 67.5)	0.11	0.74	< 0.01
NDUFB7	1.34 (0.94, 2.42)	2.10 (1.29, 3.08)	2.666	0.105	0.155
CAMK1D	34.21 (17.82, 103.44)	70.39 (35.26, 155.57)	3.045	0.083	0.030
PIK3CD	105.90 (36.69, 308.35)	333.22 (259.40, 417.90)	3.700	0.056	0.001
PSEN2	6.46 (4.44, 11.03)	8.69 (6.00, 11.67)	0.144	0.705	0.154

CRP: Colorectal polyps; CRC: Colorectal cancer; CEA: Carcinoembryonic antigen; AFP: Alpha fetoprotein; CA125: Carbohydrate antigen 125; NSE: Neuron-specific enolase; SCC: Squamous cell carcinoma; PG: Pepsinogen; ALT : Alanine aminotransferase; AST: Aspartate aminotransferase; TP: Total protein; ALB: Albumin; TB: Total bilirubin; DB: Direct bilirubin; TBA: Total bile acid; ALP: Alkaline phosphatase; GGT: γ-glutamyl transfer enzyme; Glu: Glucose; UN: Urea nitrogen; Cr: Creatinine; UA: Uric acid; CHO: Cholesterol; TG: Triglyceride esters; CK: Creatine kinase; LDH: Lactate dehydrogenase; CKMB: Creatine kinase isoenzyme; Ca: Calcium; P: Phosphorus; Mg: Magnesium; K: Potassium; Na: Sodium; Cl: Chlorine; CO_2: Carbon dioxide; LPa: Lipoprotein a; HDL: High-density lipoprotein; LDL: Low-density lipoprotein; ApoA1: Apolipoprotein A1; CYS: Cysteine; SA: sialic acid; HCY: Homocysteine; CRP: C-reactive protein; AMY: Amylase; LPS: Lipase; SOD: Superoxide dismutase; IMA: Ischemia-modified albumin.

Diagnostic value of the differential indicators between the CRP and CRC groups

Based on the 22 commonly used clinical indicators and 2 kinds of eccDNA that showed significant differences between the CRP and CRC groups, receiver operating characteristic (ROC) curves were used to evaluate the diagnostic value, as shown in Table 3. Fifteen commonly used clinical indicators and 2 kinds of eccDNA (IMA, CEA, SA, LPa, CK, TB, HDL, NSE, ALT, Ferr, DB, CA125, LDH, AMY, CY211, *CAMK1D* and *PIK3CD*) showed statistically significant differences in the area under the curve ($P < 0.05$) while the other 7 commonly used clinical indicators (CA724, HCY, CHO, P, LDL, Cl and CKMB) showed no significant difference. Therefore, 15 commonly used clinical indicators and 2 kinds of eccDNA with significant differences between the groups and the areas under the ROC curve were selected for subsequent multiparameter combined auxiliary diagnosis model analysis.

Univariate logistic regression and multivariate logistic regression analysis

Indices with statistically significant differences between the CRP and CRC groups and the ROC included IMA, CEA, SA, LP (a), CK, TB, HDL, NSE, ALT, Ferr, DB, CA125, LDH, AMY, CY211, *CAMK1D* and *PIK3CD* ($P < 0.05$). First, univariate logistic regression analysis was performed, as shown in Table 4. The Exp (B)s of CEA, IMA, SA, E3 and LPa were significantly different ($P < 0.05$), while that of CK, TB, HDL, NSE, CHO, P, LDL, Cl, CKMB and *CAMK1D* were not significantly different. Second, multivariate logistic regression analysis was performed on the differences in CEA, IMA, SA, E3 and LPa. As shown in Table 5, the Exp (B)s were significantly different for all of them ($P < 0.05$). CEA, IMA, SA, *PIK3CD* and LPa were included in the subsequent multiparameter joint auxiliary diagnosis model.

Multiparameter combined auxiliary diagnosis model building

Based on CEA, IMA, SA, *PIK3CD* and LPa, a multiparameter combined auxiliary diagnosis model was built to distinguish the 59 CRP group and 101 CRC group (including 38 cases of early CRC and 63 cases of advanced CRC).

As shown in Table 6, binary logistic regression analysis based on CEA, IMA, SA, *PIK3CD* and LPa showed that the correct rate of CRP was 76.3%, the correct rate of CRC was 85.1%, and the overall accuracy was 81.9%. The predicted probability of each sample was used as an independent variable, as shown in Figure 1A, and the AUC was 0.900 (0.855-0.946).

The discriminant analysis based on CEA, IMA, SA, *PIK3CD* and LPa showed that the correct rate of CRP was 86.4%, the correct rate of CRC was 69.3%, and the overall accuracy was 75.6%. Taking the predicted probability of each sample as an independent variable, as shown in Figure 1B, the AUC was 0.855 (0.794-0.916).

Table 3 Evaluation of the diagnostic value of 26 commonly used clinical indicators with statistical differences (colon polyp group vs colorectal cancer group)

Indicator	AUC	SE	*P* value	95% CI	
				Lower	Upper
IMA	0.787	0.036	< 0.001	0.716	0.859
CEA	0.734	0.038	< 0.001	0.658	0.809
SA	0.728	0.039	< 0.001	0.651	0.804
LPa	0.715	0.042	< 0.001	0.633	0.797
CK	0.702	0.042	< 0.001	0.619	0.784
TB	0.672	0.044	< 0.001	0.585	0.758
HDL	0.670	0.044	< 0.001	0.583	0.758
NSE	0.668	0.044	< 0.001	0.580	0.755
ALT	0.667	0.044	< 0.001	0.580	0.754
Ferr	0.663	0.045	0.001	0.575	0.751
DB	0.646	0.044	0.002	0.559	0.733
CA125	0.642	0.044	0.003	0.557	0.728
LDH	0.621	0.045	0.011	0.534	0.709
AMY	0.611	0.045	0.019	0.522	0.700
CY211	0.602	0.046	0.032	0.513	0.691
CA724	0.583	0.046	0.081	0.492	0.673
HCY	0.570	0.048	0.138	0.476	0.664
CHO	0.556	0.046	0.240	0.465	0.646
P	0.543	0.047	0.361	0.451	0.636
LDL	0.536	0.046	0.453	0.445	0.626
Cl	0.525	0.047	0.603	0.432	0.618
CKMB	0.516	0.047	0.736	0.424	0.608
CAMK1D	0.652	0.046	0.001	0.561	0.742
PIK3CD	0.753	0.047	< 0.001	0.660	0.845

AUC: Area under the curve; CEA: Carcinoembryonic antigen; AFP: Alpha fetoprotein; CA125: Carbohydrate antigen 125; NSE: Neuron-specific enolase; PG: Pepsinogen; ALT : Alanine aminotransferase; AST: Aspartate aminotransferase; TP: Total protein; ALB: Albumin; TB: Total bilirubin; DB: Direct bilirubin; TBA: Total bile acid; ALP: Alkaline phosphatase; GGT: γ-glutamyl transfer enzyme; CK: Creatine kinase; LDH: Lactate dehydrogenase; CKMB: Creatine kinase isoenzyme; Ca: Calcium; P: Phosphorus; Cl: Chlorine; LPa: Lipoprotein a; HDL: High-density lipoprotein; LDL: Low-density lipoprotein; ApoA1: Apolipoprotein A1; CYS: Cysteine; SA: sialic acid; HCY: Homocysteine; CRP: C-reactive protein; AMY: Amylase; IMA: Ischemia-modified albumin.

In the classification tree analysis based on CEA, IMA, SA, *PIK3CD* and LPa, the final independent variables included CEA, IMA, SA, *PIK3CD* and LPa, the number of nodes was 3, the number of terminal nodes was 2, and the depth was 1. Among them, the correct rate of CRP was 91.5%, the correct rate of CRC was 58.4%, and the overall accuracy rate was 70.6%. Taking the predicted probability of each sample as an independent variable, as shown in Figure 1C, the AUC was 0.750 (0.674-0.826).

The artificial neural network analysis based on CEA, IMA, SA, *PIK3CD* and LPa, CEA, IMA, SA, *PIK3CD* and LPa all entered the input layer. The number of hidden layers included 1 Layer, and the output layer included 2 Layers. The training set included 39 cases of CRP and 70 cases of CRC, among which the correct rate of identifying healthy controls was 79.5%, the correct rate of identifying colorectal cancer was 97.1%, and the overall accuracy rate was 90.8%. The test set included 20 cases of CRP and 31 cases of CRC, among which the correct rate of identifying CRP was 90.0%, the correct rate of identifying CRC was 87.1%, and the overall accuracy rate was 88.2%. Taking the predicted probability of each sample as an independent variable, as shown in Figure 1D, the AUC was 0.959 (0.934-0.985).

Table 4 Univariate Logistic Regression Analysis between the colon polyp group and the colorectal cancer group with statistically significant between-group and receiver operating characteristic indicators

Indicator	B	SE	Wals	*P* value	Exp (B)	95% CI	
						Lower	Upper
CEA	0.335	0.138	5.864	0.015	1.398	1.066	1.834
IMA	-0.138	0.048	8.352	0.004	0.871	0.793	0.956
SA	0.078	0.034	5.347	0.021	1.081	1.012	1.155
LPa	0.085	0.027	9.844	0.002	1.089	1.032	1.148
CK	-0.004	0.008	0.207	0.649	0.996	0.980	1.013
TB	-0.065	0.054	1.463	0.226	0.937	0.843	1.041
HDL	-0.949	0.822	1.331	0.249	0.387	0.077	1.941
NSE	0.160	0.084	3.656	0.056	1.174	0.996	1.383
CHO	-0.004	0.017	0.053	0.817	0.996	0.964	1.029
P	0.886	1.104	0.644	0.422	2.426	0.279	21.139
LDL	0-.585	0.368	2.534	0.111	0.557	0.271	1.145
Cl	0.112	0.086	1.682	0.195	1.119	0.944	1.325
CKMB	-0.025	0.057	0.202	0.653	0.975	0.872	1.089
CAMK1D	0.003	0.003	1.189	0.275	1.003	0.998	1.009
PIK3CD	0.003	0.001	4.429	0.035	1.003	1.000	1.005

CEA: Carcinoembryonic antigen; TB: Total bilirubin; CKMB: Creatine kinase isoenzyme; P: Phosphorus; Cl: Chlorine; LPa: Lipoprotein a; HDL: High-density lipoprotein; LDL: Low-density lipoprotein; SA: sialic acid; IMA: Ischemia-modified albumin.

Table 5 Multivariate Logistic Regreesion Analysis Exp (B) Indicators with Statistical Differences (Colon polyp group *vs* colorectal group)

Indicator	B	SE	Wals	*P* value	Exp (B)	95% CI	
						Lower	Upper
CEA	0.326	0.109	8.904	0.003	1.385	1.118	1.716
IMA	-0.136	0.035	14.765	< 0.001	0.873	0.815	0.936
SA	0.092	0.027	11.601	0.001	1.097	1.040	1.156
PIK3CD	0.002	0.001	5.852	0.016	1.002	1.000	1.004
LPa	0.064	0.022	8.888	0.003	1.066	1.022	1.112

CEA: Carcinoembryonic antigen; IMA: Ischemia-modified albumin; LPa: Lipoprotein a; SA: sialic acid.

Optimal multiparameter combined auxiliary diagnosis model selection and diagnostic evaluation

Based on CEA, IMA, SA, *PIK3CD* and LPa, binary logistic regression analysis, discriminant analysis, classification tree and neural network were used to predict the CRP and CRC groups, and the accuracy rates were 81.9%, 75.6%, 70.6%, and 90.8%, respectively. Therefore, we chose the neural network as the optimal multiparameter joint auxiliary diagnosis model. As shown above, the overall accuracy rate was 90.8%, as shown in Figure 2A. The area under the curve was 0.959 (0.934-0.985), and the sensitivity and specificity were 91.5% and 82.2%, respectively. As shown in Figure 2B, when the CRP and early CRC groups were differentiated, the area under the curve was 0.956 (0.921-0.992), and the sensitivity and specificity were 89.8% and 86.8%, respectively. As shown in Figure 2C, when the CRP and advanced CRC groups were differentiated, the area under the curve was 0.961 (0.932-0.990), and the sensitivity and specificity were 88.1% and 87.3%, respectively.

Table 6 Multi-parameter combined auxiliary diagnosis model building

Observed	Predicted		
	CRP	CRC	Correct percentage
Binary logistic regression analysis building			
CRP	45	14	76.30%
CRC	15	86	85.10%
Total percentage			81.90%
Discriminant analysis building			
CRP	51	8	86.40%
CRC	31	70	69.30%
Total percentage			75.60%
Classification tree building			
CRP	54	5	91.50%
CRC	42	59	58.40%
Total percentage			70.60%
Neural network building			
CRP	31	8	79.50%
CRC	2	68	97.10%
Total percentage			90.80%
Neural network validation			
CRP	18	2	90.00%
CRC	4	27	87.10%
Total percentage			88.20%

CRP: Colorectal polyps; CRC: Colorectal cancer.

Validation of the multi-index joint auxiliary diagnosis model

For distinguishing the CRP group from the CRC group, after comparing the multiple multiparameter joint analysis methods, the neural network based on CEA, IMA, SA, *PIK3CD* and LPa was the optimal multiparameter joint auxiliary diagnosis model. Thirty independent CRP patients and 62 CRC patients (32 in the early-stage CRC group and 30 in the advanced CRC group) were enrolled to validate the model. After validation, as shown in Figure 3A, for distinguishing CRP and CRC, the area under the curve of the neural network for CEA, IMA, SA, *PIK3CD* and LPa was 0.965 (0.930-1.000), its sensitivity and specificity were 66.1% and 70.0%, the area under the curve of the commonly used clinical indicator CEA was 0.723 (0.622-0.823), and its sensitivity and specificity were 96.8% and 86.7%, respectively. As shown in Figure 3B, for distinguishing CRP and 32 early-stage CRC, the area under the curve of the neural network model was 0.960 (0.916-1.000), with a sensitivity and specificity of 87.5% and 90.0%, the area under the curve of the commonly used clinical indicator CEA was 0.684 (0.548-0.821), and its sensitivity and specificity were 62.5% and 60.0%, respectively. As shown in Figure 3C, for distinguishing CRP and advanced CRC patients, the area under the curve of the neural network model was 0.970 (0.936, 1.000), with a sensitivity and specificity of 96.7% and 86.7%, the area under the curve of the commonly used clinical indicator CEA was 0.763 (0.632-0.895), and its sensitivity and specificity were 76.7% and 63.3%, respectively.

DISCUSSION

A biomarker is a biological molecule found in blood, other body fluids, or tissues that is a marker of a normal or abnormal process or disease. Biomarkers are primarily based on DNA, RNA, microRNA (miRNA), epigenetic changes, or antibodies. The term tumor marker, considered by some researchers to be synonymous with biomarkers, refers to substances that represent biological structures (most typically proteins, glycolipids) that can be attributed to normal cell development or to different stages of cell

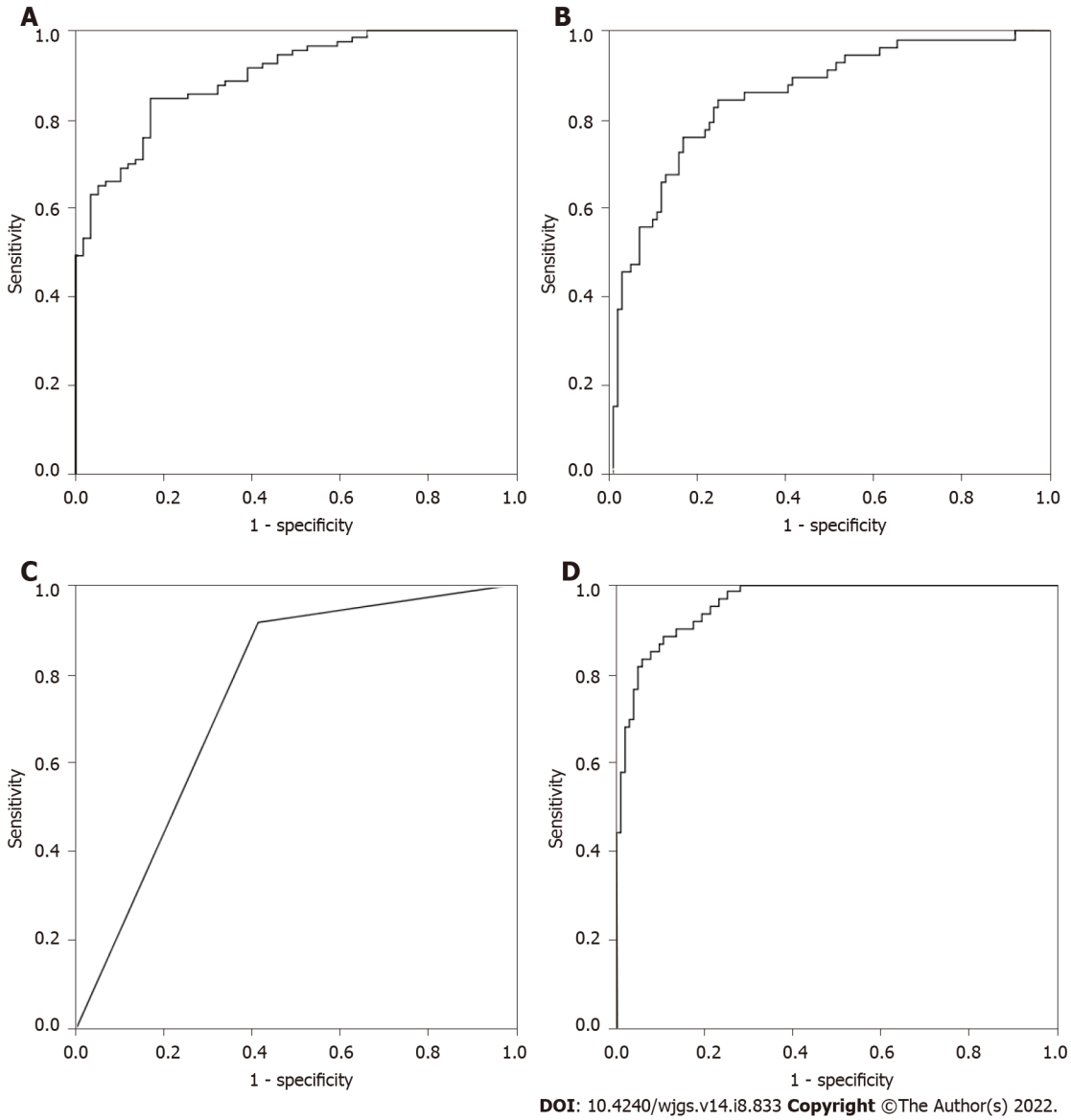

DOI: 10.4240/wjgs.v14.i8.833 **Copyright** ©The Author(s) 2022.

Figure 1 Diagnostic evaluation of multi-parameter combined auxiliary diagnosis model building. A: Binary logistic regression analysis; B: Discriminant analysis; C: Classification tree analysis; D: Neural network.

development. For example, carcinogenesis-associated antigens (TAAs) are the largest group of clinically meaningful markers. Therefore, the concentration of TAA usually correlates with the quantity (or quality) of specific tumor cells.

Discovered 50 years ago in 1965, CEA is still the only tumor marker with proven efficacy in monitoring treatment in CRC patients. CEA was initially thought to be CRC specific, but elevated CEA levels have since been detected in other tumors, *e.g.*, gastric and pancreatic cancer, and inflammatory states. Rarely, elevated CEA concentrations are found in CRC stage I[16]. Furthermore, CEA cannot differentiate between benign and malignant polyps. Recently, several studies have explored the advantages of mRNA molecules encoding CEA for the detection of CRC, but the results were not superior to CEA[17]. In some studies, high CEA concentrations in patients with CRC stages II and III may be indicative of a more aggressive cancer type. CEA is the marker of choice for monitoring disseminated disease during systemic therapy. Sustained increases in CEA levels are often associated with disease progression, even though radiological examination may prove otherwise. However, chemotherapy may also cause a temporary increase in CEA concentrations, which must be taken into account. Therefore, it is not recommended to measure CEA levels within 2 wk after chemotherapy but only after 4 to 6 wk in oxaliplatin-treated patients. Cancer antigen 19-9 (CA 19-9) is a glycoprotein whose relevance in the diagnosis of CRC remains unclear. Most investigators concluded that the sensitivity of CA 19-9 was much lower than that of CEA and that elevated CA 19-9 Levels indicated a poor prognosis[18]. Other carbohydrate antigens, CA 19-5 and CA 50, have also been investigated with relatively disappointing results. CA 72-4 is a biomarker with poor sensitivity, ranging from 9% to 31%, and good specificity, ranging from 89% to 95%, for screening patients for CRC. The diagnostic

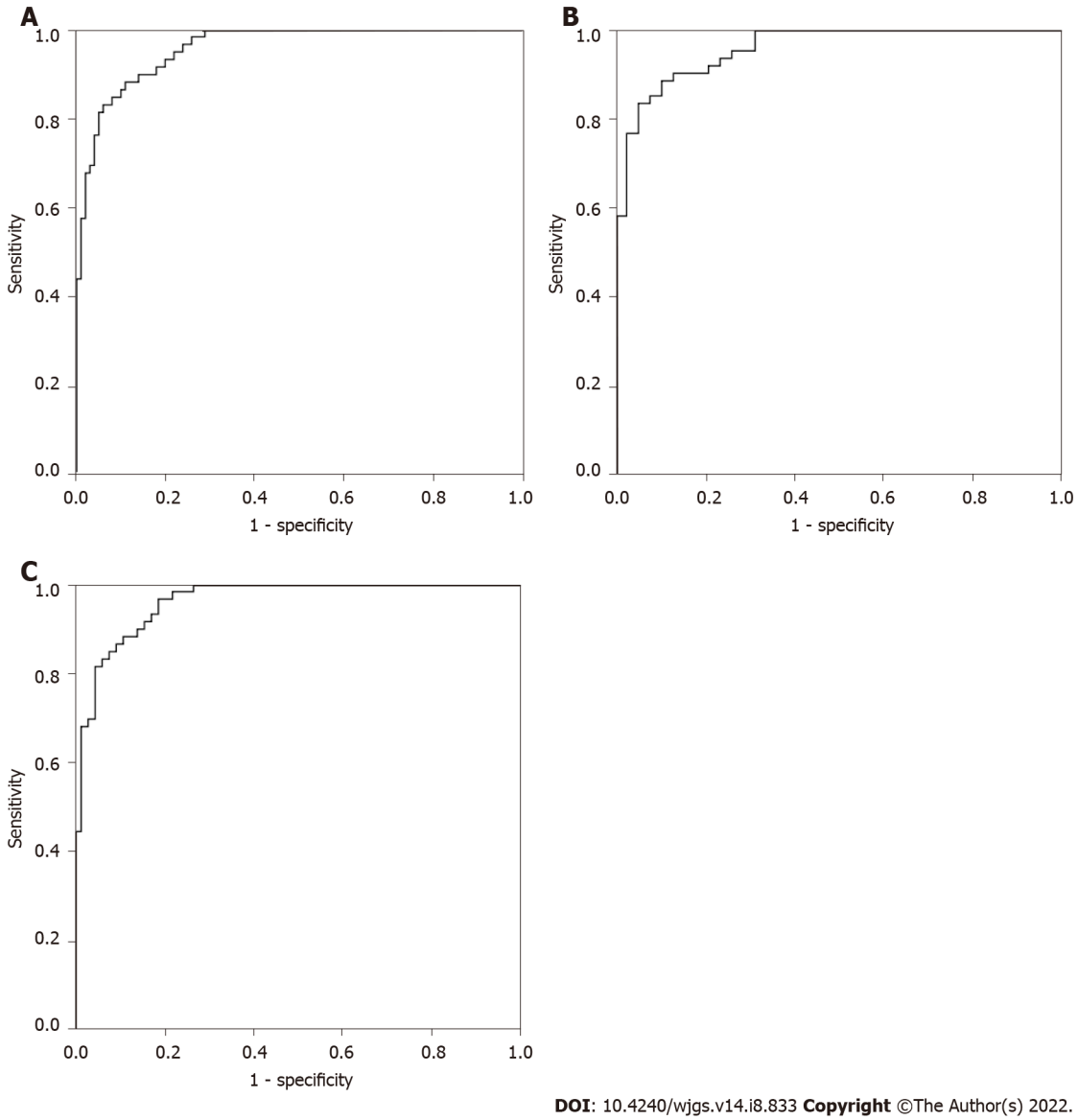

DOI: 10.4240/wjgs.v14.i8.833

Figure 2 Diagnostic evaluation of the neural network multi-parameter diagnostic model building. A: Colorectal polyps (CRP) *vs* colorectal cancer (CRC); B: CRP *vs* early stage of CRC; C: CRP *vs* advanced stage of CRC.

information provided by CA 72-4 in recurrent CRC is borderline and far inferior to that of CEA. There is a consensus that CA 72-4 has a rather low sensitivity and incomplete specificity in the screening and follow-up of CRC patients[19]. Tissue polypeptide-specific antigen (TPS) and tissue polypeptide antigen (TPA), which detect cytokeratin 8, 18, and 19 fragments, are not recommended for CRC screening due to their lack of sensitivity and specificity. Most investigators found that elevated levels of TPA and TPS were observed in the metastatic stage of CRC. Further studies showed that the combination of TPA and CEA improved the sensitivity of these biomarkers in identifying patients with CRC recurrence. Other biomarkers, such as thymidine phosphorylase and DNA ploidy, were found to have no utility in the detection, staging or follow-up of CRC patients.

NDUFB is an accessory subunit of *NADH* dehydrogenase (com-plex I) of the mitochondrial membrane respiratory chain, encoded by nuclear genes[20]. Mutations in *NDUFB* may promote tumor metastasis[21]. In addition, a SNP (rs7830235) associated with prostate cancer risk is located in the *NDUFB* gene[22]. In addition to this, most of the other subunits of *NADH* dehydrogenase (*NDUFB1-8/11*) family were found to have significant prognostic value (DMFS) in breast cancer patients, and it was the mainstay of MDA-MB-231 breast cancer cell proliferation, inhibition of migration and invasion [23]. Its high expression is positively correlated with the prognosis of gastric cancer, suggesting that these proteins may serve as new candidate diagnostic and prognostic biomarkers for gastric cancer[24]. *CAMK1D* is a member of the calcium/calmodulin-dependent protein kinase 1 family[25]. It involved in a variety of physiological processes, including activation of CREB-dependent gene transcription, differentiation and activation of neutrophils, and regulation of apoptosis in erythrocytic leukemia[26]. Recent studies have shown that overexpression of *CAMK1D* can promote the proliferation of breast cancer[27].

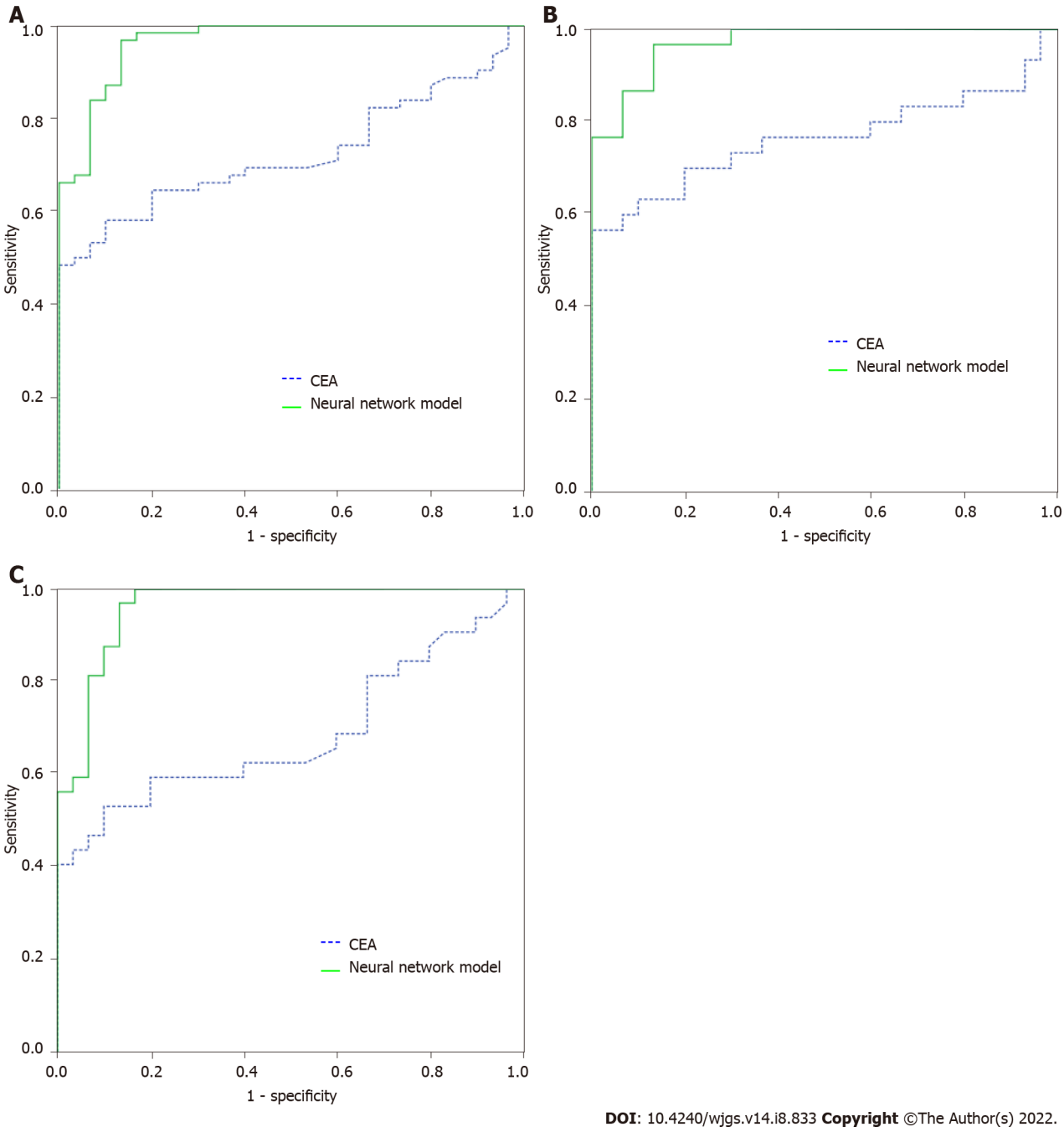

DOI: 10.4240/wjgs.v14.i8.833

Figure 3 Diagnostic evaluation of the neural network multi-parameter diagnostic model and carcinoembryonic antigen validation. A: Colorectal polyps (CRP) *vs* colorectal cancer (CRC); B: CRP *vs* early stage of CRC; C: CRP *vs* advanced stage of CRC. CEA: Carcinoembryonic antigen.

Knockdown of *CAMK1D* in HT-29 and SW480 cells significantly reduced cell proliferation, invasion/migration capacity, and significantly increased apoptosis[28]. Activation of phosphoinositide 3-kinase (PI3K) signaling is one of the most common events in several human cancers, including CRC. PI3K is a family of lipid kinases that phosphorylate phosphatidylinositol 4, 5-bisphosphate to generate phosphatidylinositol-3, 4, 5-triphosphate, which in turn activates serine-threonine[29-31]. PI3Ks are classified into 3 classes according to their substrate specificity and structure in mammals. Of these, class I PI3Ks appear to be most associated with human cancers. Class I PI3Ks are further divided into subclasses IA and IB based on their adapters. Class IA PI3Ks contain a p110 catalytic subunit and a p85 regulatory subunit. The class IA catalytic isoforms p110α, p110β and p110δ are encoded by the genes *PIK3CA*, *PIK3CB* and *PIK3CD*, respectively. *PIK3CB* and *PIK3CD* are often overexpressed or amplified in cancer[32,33]. *PIK3CD* is mainly expressed in leukocytes and plays a key role in some hematological malignancies. Furthermore, *PIK3CD* has recently been associated with several human solid tumors, including hepatocellular carcinoma, glioma, glioblastoma, neuroblastoma, and breast cancer[33,34]. *PIK3CD* induces cell growth and invasion in colorectal cancer by activating AKT/GSK-3β/β-catenin signaling[35]. Presenilin 2 (*PSEN2*) is a protein-coding gene. Diseases associated with *PSEN2* include

Alzheimer's disease[36]. Its related pathways include EPH-Ephrin signaling and p75 NTR receptor-mediated signaling. Presenilin (*PSEN1* or *PSEN2*) mutations are generally thought to be present in Alzheimer's disease patients with inherited disorders[37,38]. Although We have built a multi-parameter neural network diagnostic model for CRC, however, multi-centers and larger sample size still needed in the future study.

CONCLUSION

In conclusion, we built a multi-parameter neural network diagnostic model included CEA, IMA, SA, *PIK3CD* and LPa for early detection of CRC, compared to the conventional CEA, it showed significant improvement.

ARTICLE HIGHLIGHTS

Research background

Most patients with colorectal cancer (CRC) are diagnosed at an advanced stage. The high morbidity and mortality of advanced CRC indicates an urgent need for clinical improvements in early CRC detection and individualized management.

Research motivation

Early detection of CRC is urgently needed in clinical practice. Commonly biomarker and extra-chromosomal circular DNA (eccDNA) may have potential diagnostic value for CRC.

Research objectives

This study aimed to build a multi-parameter diagnostic model for early detection of CRC.

Research methods

Total 59 colorectal polyps (CRP) groups, and 101 CRC patients (38 early-stage CRC and 63 advanced CRC) for model establishment. In addition, 30 CRP groups, and 62 CRC patients (30 early-stage CRC and 32 advanced CRC) were separately included to validate the model. 51 commonly used clinical detection indicators and the 4 eccDNA markers *NDUFB7*, *CAMK1D*, *PIK3CD* and *PSEN2* that we screened earlier. Four multi-parameter joint analysis methods: binary logistic regression analysis, discriminant analysis, classification tree and neural network to establish a multi-parameter joint diagnosis model.

Research results

Neural network included carcinoembryonic antigen (CEA), ischemia-modified albumin (IMA), sialic acid (SA), *PIK3CD* and lipoprotein a (LPa) was chosen as the optimal multi-parameter combined auxiliary diagnosis model to distinguish CRP and CRC group, when it differentiated 59 CRP and 101 CRC, its overall accuracy was 90.8%, its area under the curve (AUC) was 0.959 (0.934, 0.985), and the sensitivity and specificity were 91.5% and 82.2%, respectively. After validation, when distinguishing based on 30 CRP and 62 CRC patients, the AUC was 0.965 (0.930, 1.000), and its sensitivity and specificity were 66.1% and 70.0%. When distinguishing based on 30 CRP and 32 early-stage CRC patients, the AUC was 0.960 (0.916, 1.000), with a sensitivity and specificity of 87.5% and 90.0%, distinguishing based on 30 CRP and 30 advanced CRC patients, the AUC was 0.970 (0.936, 1.000), with a sensitivity and specificity of 96.7% and 86.7%.

Research conclusions

We built a multi-parameter neural network diagnostic model included CEA, IMA, SA, *PIK3CD* and LPa for early detection of CRC, compared to the conventional CEA, it showed significant improvement.

Research perspectives

Larger sample size and multi-center study should be performed to validate the diagnostic model in future studies.

FOOTNOTES

Author contributions: Li J and Xian GA designed the study; Li J, Ren ZC and Jiang T performed the research; Li J, Wang ZL and Jiang T analyzed the date; Li J wrote the paper; Xiang GA and Zhang PJ revised the manuscript for final submission; Li J and Jiang T contributed equally to this study; Zhang PJ and Xiang GA the co-corresponding

author.

Supported by National Natural Science Foundation of China, No. 81972010; National Key Research and Development Program of China, No. 2020YFC2002700; National Key Research and Development Program of China, No. 2020YFC2004604.

Institutional review board statement: The study was reviewed and approved by the Chinese PLA General Hospital Review Board.

Informed consent statement: All study participants, or their legal guardian, provided informed written consent prior to study enrollment.

Conflict-of-interest statement: We declare that we have no financial or personal relationships with other individuals or organizations that can inappropriately influence our work and that there is no professional or other personal interest of any nature in any product, service and/or company that could be construed as influencing the position presented in or the review of the manuscript.

Data sharing statement: No data was to share.

Country/Territory of origin: China

ORCID number: Jian Li 0000-0002-2168-4240; Tao Jiang 0000-0002-2127-9085; Zeng-Ci Ren 0000-0002-0931-3535; Zhen-Lei Wang 0000-0001-7126-9136; Peng-Jun Zhang 0000-0002-7391-2495; Guo-An Xiang 0000-0002-4218-6160.

S-Editor: Wang JL
L-Editor: A
P-Editor: Wang JL

REFERENCES

1 **Kuipers EJ**, Grady WM, Lieberman D, Seufferlein T, Sung JJ, Boelens PG, van de Velde CJ, Watanabe T. Colorectal cancer. *Nat Rev Dis Primers* 2015; **1**: 15065 [PMID: 27189416 DOI: 10.1038/nrdp.2015.65]
2 **Cho YA**, Lee J, Oh JH, Chang HJ, Sohn DK, Shin A, Kim J. Genetic Risk Score, Combined Lifestyle Factors and Risk of Colorectal Cancer. *Cancer Res Treat* 2019; **51**: 1033-1040 [PMID: 30336659 DOI: 10.4143/crt.2018.447]
3 **Mader S**, Pantel K. Liquid Biopsy: Current Status and Future Perspectives. *Oncol Res Treat* 2017; **40**: 404-408 [PMID: 28693023 DOI: 10.1159/000478018]
4 **Alix-Panabières C**, Pantel K. Liquid Biopsy: From Discovery to Clinical Application. *Cancer Discov* 2021; **11**: 858-873 [PMID: 33811121 DOI: 10.1158/2159-8290.CD-20-1311]
5 **Poulet G**, Massias J, Taly V. Liquid Biopsy: General Concepts. *Acta Cytol* 2019; **63**: 449-455 [PMID: 31091522 DOI: 10.1159/000499337]
6 **Mazumder S**, Datta S, Ray JG, Chaudhuri K, Chatterjee R. Liquid biopsy: miRNA as a potential biomarker in oral cancer. *Cancer Epidemiol* 2019; **58**: 137-145 [PMID: 30579238 DOI: 10.1016/j.canep.2018.12.008]
7 **Junqueira-Neto S**, Batista IA, Costa JL, Melo SA. Liquid Biopsy beyond Circulating Tumor Cells and Cell-Free DNA. *Acta Cytol* 2019; **63**: 479-488 [PMID: 30783027 DOI: 10.1159/000493969]
8 **Tay TKY**, Tan PH. Liquid Biopsy in Breast Cancer: A Focused Review. *Arch Pathol Lab Med* 2021; **145**: 678-686 [PMID: 32045277 DOI: 10.5858/arpa.2019-0559-RA]
9 **Ye Q**, Ling S, Zheng S, Xu X. Liquid biopsy in hepatocellular carcinoma: circulating tumor cells and circulating tumor DNA. *Mol Cancer* 2019; **18**: 114 [PMID: 31269959 DOI: 10.1186/s12943-019-1043-x]
10 **Giannopoulou L**, Zavridou M, Kasimir-Bauer S, Lianidou ES. Liquid biopsy in ovarian cancer: the potential of circulating miRNAs and exosomes. *Transl Res* 2019; **205**: 77-91 [PMID: 30391474 DOI: 10.1016/j.trsl.2018.10.003]
11 **Chen M**, Zhao H. Next-generation sequencing in liquid biopsy: cancer screening and early detection. *Hum Genomics* 2019; **13**: 34 [PMID: 31370908 DOI: 10.1186/s40246-019-0220-8]
12 **Kumar P**, Kiran S, Saha S, Su Z, Paulsen T, Chatrath A, Shibata Y, Shibata E, Dutta A. ATAC-seq identifies thousands of extrachromosomal circular DNA in cancer and cell lines. *Sci Adv* 2020; **6**: eaba2489 [PMID: 32440553 DOI: 10.1126/sciadv.aba2489]
13 **Su Z**, Saha S, Paulsen T, Kumar P, Dutta A. ATAC-Seq-based Identification of Extrachromosomal Circular DNA in Mammalian Cells and Its Validation Using Inverse PCR and FISH. *Bio Protoc* 2021; **11**: e4003 [PMID: 34124304 DOI: 10.21769/BioProtoc.4003]
14 **Wang M**, Chen X, Yu F, Ding H, Zhang Y, Wang K. Extrachromosomal Circular DNAs: Origin, formation and emerging function in Cancer. *Int J Biol Sci* 2021; **17**: 1010-1025 [PMID: 33867825 DOI: 10.7150/ijbs.54614]

15 **Wang T**, Zhang H, Zhou Y, Shi J. Extrachromosomal circular DNA: a new potential role in cancer progression. *J Transl Med* 2021; **19**: 257 [PMID: 34112178 DOI: 10.1186/s12967-021-02927-x]

16 **Thirunavukarasu P**, Sukumar S, Sathaiah M, Mahan M, Pragatheeshwar KD, Pingpank JF, Zeh H 3rd, Bartels CJ, Lee KK, Bartlett DL. C-stage in colon cancer: implications of carcinoembryonic antigen biomarker in staging, prognosis, and management. *J Natl Cancer Inst* 2011; **103**: 689-697 [PMID: 21421861 DOI: 10.1093/jnci/djr078]

17 **Goldstein MJ**, Mitchell EP. Carcinoembryonic antigen in the staging and follow-up of patients with colorectal cancer. *Cancer Invest* 2005; **23**: 338-351 [PMID: 16100946 DOI: 10.1081/cnv-58878]

18 **Ballehaninna UK**, Chamberlain RS. The clinical utility of serum CA 19-9 in the diagnosis, prognosis and management of pancreatic adenocarcinoma: An evidence based appraisal. *J Gastrointest Oncol* 2012; **3**: 105-119 [PMID: 22811878 DOI: 10.3978/j.issn.2078-6891.2011.021]

19 **Carpelan-Holmström M**, Louhimo J, Stenman UH, Alfthan H, Järvinen H, Haglund C. CEA, CA 242, CA 19-9, CA 72-4 and hCGbeta in the diagnosis of recurrent colorectal cancer. *Tumour Biol* 2004; **25**: 228-234 [PMID: 15627885 DOI: 10.1159/000081385]

20 **Tan AS**, Baty JW, Berridge MV. The role of mitochondrial electron transport in tumorigenesis and metastasis. *Biochim Biophys Acta* 2014; **1840**: 1454-1463 [PMID: 24141138 DOI: 10.1016/j.bbagen.2013.10.016]

21 **Wang L**, McDonnell SK, Hebbring SJ, Cunningham JM, St Sauver J, Cerhan JR, Isaya G, Schaid DJ, Thibodeau SN. Polymorphisms in mitochondrial genes and prostate cancer risk. *Cancer Epidemiol Biomarkers Prev* 2008; **17**: 3558-3566 [PMID: 19064571 DOI: 10.1158/1055-9965.EPI-08-0434]

22 **Lin X**, Wells DE, Kimberling WJ, Kumar S. Human NDUFB9 gene: genomic organization and a possible candidate gene associated with deafness disorder mapped to chromosome 8q13. *Hum Hered* 1999; **49**: 75-80 [PMID: 10077726 DOI: 10.1159/000022848]

23 **Li LD**, Sun HF, Liu XX, Gao SP, Jiang HL, Hu X, Jin W. Down-Regulation of NDUFB9 Promotes Breast Cancer Cell Proliferation, Metastasis by Mediating Mitochondrial Metabolism. *PLoS One* 2015; **10**: e0144441 [PMID: 26641458 DOI: 10.1371/journal.pone.0144441]

24 **Su F**, Zhou FF, Zhang T, Wang DW, Zhao D, Hou XM, Feng MH. Quantitative proteomics identified 3 oxidative phosphorylation genes with clinical prognostic significance in gastric cancer. *J Cell Mol Med* 2020; **24**: 10842-10854 [PMID: 32757436 DOI: 10.1111/jcmm.15712]

25 **Yamada T**, Suzuki M, Satoh H, Kihara-Negishi F, Nakano H, Oikawa T. Effects of PU.1-induced mouse calcium-calmodulin-dependent kinase I-like kinase (CKLiK) on apoptosis of murine erythroleukemia cells. *Exp Cell Res* 2004; **294**: 39-50 [PMID: 14980499 DOI: 10.1016/j.yexcr.2003.10.023]

26 **Gaines P**, Lamoureux J, Marisetty A, Chi J, Berliner N. A cascade of Ca (2+)/calmodulin-dependent protein kinases regulates the differentiation and functional activation of murine neutrophils. *Exp Hematol* 2008; **36**: 832-844 [PMID: 18400360 DOI: 10.1016/j.exphem.2008.02.009]

27 **Bergamaschi A**, Kim YH, Kwei KA, La Choi Y, Bocanegra M, Langerød A, Han W, Noh DY, Huntsman DG, Jeffrey SS, Børresen-Dale AL, Pollack JR. CAMK1D amplification implicated in epithelial-mesenchymal transition in basal-like breast cancer. *Mol Oncol* 2008; **2**: 327-339 [PMID: 19383354 DOI: 10.1016/j.molonc.2008.09.004]

28 **Liu W**, Li S. LncRNA ILF3-AS1 Promotes the Progression of Colon Adenocarcinoma Cells Through the miR-619-5p/CAMK1D Axis. *Onco Targets Ther* 2021; **14**: 1861-1872 [PMID: 33737811 DOI: 10.2147/OTT.S296441]

29 **Fruman DA**, Rommel C. PI3K and cancer: lessons, challenges and opportunities. *Nat Rev Drug Discov* 2014; **13**: 140-156 [PMID: 24481312 DOI: 10.1038/nrd4204]

30 **Thorpe LM**, Yuzugullu H, Zhao JJ. PI3K in cancer: divergent roles of isoforms, modes of activation and therapeutic targeting. *Nat Rev Cancer* 2015; **15**: 7-24 [PMID: 25533673 DOI: 10.1038/nrc3860]

31 **Wang G**, Cao X, Lai S, Luo X, Feng Y, Xia X, Yen PM, Gong J, Hu J. PI3K stimulates DNA synthesis and cell-cycle progression *via* its p55PIK regulatory subunit interaction with PCNA. *Mol Cancer Ther* 2013; **12**: 2100-2109 [PMID: 23939377 DOI: 10.1158/1535-7163.MCT-12-0920]

32 **Singh P**, Dar MS, Dar MJ. p110α and p110β isoforms of PI3K signaling: are they two sides of the same coin? *FEBS Lett* 2016; **590**: 3071-3082 [PMID: 27552098 DOI: 10.1002/1873-3468.12377]

33 **Tzenaki N**, Papakonstanti EA. p110δ PI3 kinase pathway: emerging roles in cancer. *Front Oncol* 2013; **3**: 40 [PMID: 23459844 DOI: 10.3389/fonc.2013.00040]

34 **Fang Y**, Xue JL, Shen Q, Chen J, Tian L. MicroRNA-7 inhibits tumor growth and metastasis by targeting the phosphoinositide 3-kinase/Akt pathway in hepatocellular carcinoma. *Hepatology* 2012; **55**: 1852-1862 [PMID: 22234835 DOI: 10.1002/hep.25576]

35 **Chen JS**, Huang JQ, Luo B, Dong SH, Wang RC, Jiang ZK, Xie YK, Yi W, Wen GM, Zhong JF. PIK3CD induces cell growth and invasion by activating AKT/GSK-3β/β-catenin signaling in colorectal cancer. *Cancer Sci* 2019; **110**: 997-1011 [PMID: 30618098 DOI: 10.1111/cas.13931]

36 **Gan CL**, Zhang T, Lee TH. The Genetics of Alzheimer's Disease in the Chinese Population. *Int J Mol Sci* 2020; **21** [PMID: 32235595 DOI: 10.3390/ijms21072381]

37 **Xiao X**, Liu H, Liu X, Zhang W, Zhang S, Jiao B. *APP*, *PSEN1*, and *PSEN2* Variants in Alzheimer's Disease: Systematic Re-evaluation According to ACMG Guidelines. *Front Aging Neurosci* 2021; **13**: 695808 [PMID: 34220489 DOI: 10.3389/fnagi.2021.695808]

38 **Lessard CB**, Rodriguez E, Ladd TB, Minter LM, Osborne BA, Miele L, Golde TE, Ran Y. γ-Secretase modulators exhibit selectivity for modulation of APP cleavage but inverse γ-secretase modulators do not. *Alzheimers Res Ther* 2020; **12**: 61 [PMID: 32430033 DOI: 10.1186/s13195-020-00622-5]

Published by **Baishideng Publishing Group Inc**
7041 Koll Center Parkway, Suite 160, Pleasanton, CA 94566, USA
Telephone: +1-925-3991568
E-mail: bpgoffice@wjgnet.com
Help Desk: https://www.f6publishing.com/helpdesk
https://www.wjgnet.com